General and Comparative Endocrinology 281 (2019) 105–116

Contents lists available at ScienceDirect

General and Comparative Endocrinology

journal homepage: www.elsevier.com/locate/ygcen

Bromodomain-containing protein 2 promotes lipolysis via ERK/HSL signalling pathway in white adipose tissue of mice

Jiuyu Zong[a], Shuting Li[a], Yuxiong Wang[a], Wei Mo[a], Ruixin Sun[b,*], Min Yu[a,*]

[a] The Key Laboratory of Metabolism and Molecular Medicine, The Ministry of Education, Department of Biochemistry and Molecular Biology, School of Basic Medical Science, Fudan University, Shanghai 200032, China

[b] State Key Laboratory of Oncogenes and Related Genes, Shanghai Cancer Institute, Renji Hospital, Shanghai Jiaotong University School of Medicine, Shanghai 200032, China

ARTICLE INFO

Keywords:
Brd2
Lipolysis
Free fatty acid
ERK
Insulin resistance

ABSTRACT

White adipose tissue (WAT) dysfunction is prevalent among patients with type 2 diabetes mellitus (T2DM). Uncontrolled free fatty acid (FFA) release from WAT stores has detrimental effects on lipid metabolism, leading to insulin resistance. Bromodomain-containing protein 2 (Brd2) has emerged as a central transcriptional regulator of adipocyte differentiation and pancreatic β-cell bioactivity. A recent study shows that Brd2 overexpression leads to insulin resistance in mice. However, the mechanisms underlying these effects have not been fully elucidated. This study provides the first evidence that adenoviral-mediated Brd2 overexpression in the WAT of mice increases lipolysis-related gene expression in addition to significantly reducing WAT size and promoting plasma FFA release. Brd2 overexpression in adipocytes also inhibits fat synthesis-related gene expression, while activating hormone-sensitive lipase (HSL) expression and ERK-dependent perilipin 1 inhibition as well as promoting glycerol release, which are all involved in lipolysis. Collectively, these results indicate that Brd2 triggers insulin resistance via lipolysis-mediated FFA release.

1. Introduction

Type 2 diabetes mellitus (T2DM) is a major metabolic disease associated with high morbidity and mortality worldwide (Fruci et al., 2013; Liu et al., 2017). Insulin resistance is one of the major risk factors of T2DM and is associated with an increase in plasma FFA levels (Galles et al., 2018). Notably, white adipose tissue (WAT) functions as an energy storage organ and secretes several biologically active molecules that regulate glucose and lipid metabolism. One of the major functions of WAT is to regulate lipolysis and the release of free fatty acid (FFA) into circulation (Greenberg and Obin, 2006). Previous reports have also linked dysregulated adipose tissue catabolism and abnormal FFA release to insulin resistance and T2DM development (Pal et al., 2012; Petersen et al., 2017; Titchenell et al., 2016). However, the precise molecular mechanisms underlying excessive lipolysis in adipose tissue and its relationship with insulin resistance are largely unknown.

Inappropriate increase in circulating FFA are known to promote ectopic lipid deposition in peripheral tissues, resulting in decreased glucose uptake, impaired insulin secretion from β-cells, and insulin resistance (Kahn et al., 2006; Karpe et al., 2011). Circulating FFA levels are predominantly derived from stored triglycerides that are actively broken down through enzymatic lipolysis in WAT (Bezaire et al., 2009a,b; Shostak et al., 2013). The main enzymes involved in this process are hormone-sensitive lipase (HSL), adipose triglyceride lipase (ATGL), and perilipin 1 (Bartz et al., 2007; Jaworski et al., 2007; Pinent et al., 2011). Further, the evolutionarily conserved mitogen-activated protein kinase/extracellular signal-regulated kinase (MAPK/ERK) signalling pathway is also involved in lipid metabolism (Fricke et al., 2004; Johnson and Lapadat, 2002; Wu et al., 2018), and its activation promotes the phosphorylation of HSL at Ser855 and the subsequent degradation of perilipin 1, which modulates FFA release and accelerates lipolysis (Greenberg et al., 2001; Hong et al., 2018).

A number of other factors have also been linked to lipolysis and/or insulin resistance. Bromodomain-containing protein 2 (Brd2), is a transcriptional co-activator/co-repressor that has switch mating type/sucrose non-fermenting (SWI/SNF)-like functions. Brd2 includes two

* Corresponding authors at: State Key Laboratory of Oncogenes and Related Genes, Shanghai Cancer Institute, Renji Hospital, Shanghai Jiaotong University School of Medicine, No. 25/2200 Xietu Road, Shanghai 200032, China (R. Sun). The Key Laboratory of Metabolism and Molecular Medicine, The Ministry of Education, Department of Biochemistry and Molecular Biology, School of Basic Medical Science, Fudan University, P.O. Box #238, No.138 Yi Xue Yuan Road, Shanghai 200032, China (M. Yu).

E-mail addresses: ruixinsun@shsci.org (R. Sun), minyu@shmu.edu.cn (M. Yu).

https://doi.org/10.1016/j.ygcen.2019.05.011
Received 26 February 2019; Received in revised form 17 April 2019; Accepted 14 May 2019
Available online 21 May 2019
0016-6480/ © 2019 Elsevier Inc. All rights reserved.

bromodomain functional domains (BD1 and BD2), a nuclear localization signal domain (NLS), and an ET domain (ET). The BD1 and BD2 domains contain sites for binding to acetylated histones and can exert transcriptional regulation through acetylation in the nucleus (Peng et al., 2007). Brd2 is known to regulate various cellular processes, including chromatin remodelling (Sinha et al., 2005), adipocyte differentiation (Zang et al., 2013), inflammatory responses (Belkina et al., 2013), pancreatic β-cell mass, and insulin production (Wang et al., 2009). Recent studies have also shown that disruption of Brd2 expression in mice causes severe obesity, but this loss-of-function-mutation does not appear to result in insulin resistance or T2DM (Wang et al., 2009). Alternatively, Brd2 overexpression in adipose tissue attenuates insulin sensitivity, leading to insulin resistance (Sun et al., 2017). However, while it is likely that Brd2 is involved in the dysregulation of lipid metabolism, resulting in insulin resistance and T2DM, the related signalling cascades involved in the cross-talk between WAT lipolysis and T2DM pathogenesis require additional study.

In this study, we evaluated the effects of Brd2 overexpression in vivo and in vitro to elucidate the role of this transcription factor and its associated signalling pathways in lipolysis-related insulin resistance. Our results show that Brd2 plays a critical role in regulating lipolysis in WAT through ERK/HSL pathway activation and perilipin 1 degradation, leading to accelerated FFA release. By further clarifying the specific regulation mechanism of Brd2 on lipid metabolism, we can provide a potential application of Brd2 as a therapeutic target for T2DM-associated adipocyte metabolism dysfunction.

2. Materials and methods

2.1. Materials

High glucose Dulbecco's modified Eagle's medium (DMEM) and penicillin/streptomycin were purchased from Gibco BRL (Grand Island, NY). Calf serum and foetal calf serum were obtained from Hyclone (Logan, UT). Trizol reagent, HiScript 1st Strand cDNA Sythesis Kit and SYBR Green PCR Master Mix Kit were ordered from Vazyme (NJ, CN). Adipocyte differentiation reagents dexamethasone (Dex), 1-methyl-3-isobutyxanthine (Mix), human insulin and Palmitic acid (PA) were from Sigma-Aldrich (St. Louis, MO) and U0126 was from Cell Signalling Technology (Danvers, MA).

The following antibodies were used for immunoblotting: HSL (#18381), Perilipin 1 (#9349), GAPDH (#2118), ERK (#4695), p-ERK (#4370), IRS-1 (#2382), Akt (#9272) and p-Akt (#4060) were from Cell Signalling Technology (Danvers, MA). P-HSL (Ser855) (#BS4234) was from Bioworld, and anti-Brd2 (ab139690), p-IRS-1 (ab109543) were from Abcam.

2.2. Mice

All the animal experiments in this study were approved by the Animal Care and Use Committee of Fudan University Shanghai Medical College and were performed according to the guidelines of the National Institute of Health on the care and use of laboratory animals (Publication no. 8023, revised 1978). Wild-type C57BL/6J male mice (6–8 weeks old) with similar weight and body temperature were maintained on a 12:12-h light/dark cycle at room temperature with free access to food and water. The mice were maintained for 4 weeks on a normal chow diet before being divided into two groups (n = 6 per group) that received a bilateral subcutaneous injection of either Ad-Brd2 or Ad-C in the groin. Mice were injected twice a week with the purified adenovirus for 4 weeks.

After that, we used the anal thermometer (Xinhang, Beijing) and the electronic scale (Sartourius, Germany) to measure the temperatures and weights of mice, respectively. Each mouse was tested for thrice and the average values were recorded.

2.3. RNA interference, adenoviral expression vectors and infection

Brd2 shRNA construction was performed as described previously (Sun et al., 2017). We used Gateway technology to increase Brd2 overexpression. We first generated a Brd2 expression vector using Brd2 cDNA obtained from 3T3-L1 pre-adipocytes, and then used the ViraPower adenoviral expression system (Invitrogen, Carlsbad, CA, USA) to construct a recombinant Brd2 adenovirus (Ad-Brd2) and a negative control adenovirus (Ad-C). The blunt-ended PCR products were cloned into the pENTR-TOPO vector via an LR recombination reaction. Ad-Brd2 and Ad-C vectors were amplified in 293A cells and purified using the Vivapure AdenoPACK adenovirus purification kit (Sartorius, Gottingen, Germany).

2.4. Construction of deletion mutant vector

We used the lentiviral vector pCDH-CMV-MCS-EF1-puro to construct four Brd2 mutants. Using the mouse genomic cDNA library, Brd2 protein domain deletion mutant vectors were obtained through two rounds of PCR, including mutants that lack histone acetylation sites: BD1 deletion (pMSCV-ΔBD1), BD2 deletion (pMSCV-ΔBD2), BD1 & BD2 Deletions (pMSCV-ΔBD1&ΔBD2); a mutant that is only expressed in the cytoplasm: NLS nuclear localization signal fragment deletion (pMSCV-ΔNLS). We constructed Brd2 overexpression plasmid by searching the cDNA library (pMSCV-Brd2) and used untreated vectors as wild type (pMSCV-C). We transfected the mutated plasmids into 293 T cells respectively. After 72 h, the virus supernatants were collected and infected with 3T3-L1 mature adipocytes. Samples were collected after 72 h. PCR primers are shown in Table 1.

2.5. Haematoxylin and eosin (H&E) staining

Standard H&E staining was performed on 5-μm paraffin sections of WAT. The cell diameter was measured with Image J software from H&E-stained sections of 3 individual samples in each group.

2.6. Enzyme-linked immunosorbent assay (ELISA)

The mice were anesthetized after the last injection of Ad-Brd2 or Ad-C by an intraperitoneal injection with 10% chloral hydrate. Then, the blood was obtained by removing the eyeballs of the normal diet mice (feed state). After that the mice were sacrificed by dislocating the cervical vertebra. Blood samples were collected using heparin as an anticoagulant. To obtain plasma samples, the blood samples were centrifuged for 15 min at 1000 × *g* for 30 min, and then the obtained plasma samples were diluted with a diluent at a ratio of 1:2 to a final

Table 1
Specific design of primer sequences for construction of Brd2 protein domain deletion mutation vectors.

Gene	Forward primer (5′-3′)	Reverse primer (5′-3′)
ΔBD1	TCTTGTGGTCCTGGCTTTTTGGGATTGGACACCT	AGCCAGGACCACAAGAGGAGCAAGAGCTTGTGGT
ΔBD2	ATCTTGGCCTCTGACAGCTTCCCTTTCTTAGAGC	TGTCAGAGGCCAAGATGCCAGATGAGCCACTGGA
ΔBD1&ΔBD2	TTCTCTGCTTTTTCCTTTTTCTCTCTCTTCCGCT	AGGAAAAAGCAGAGAAACATCGTGGCCGAATTGG
ΔNLS	CCGCTCGAATGCTGCAAAACGTGACT	CCGGAATTCTTAGCCCGAGTCTGAATCG

volume of 50 μl per well in 96-well plates. The plasma FFA levels were then determined by FFA (ELISA) test kit (Quansys Bioscience, Logan, UT).

2.7. Glycerol release assay

Collected the plasma and inguinal subcutaneous adipose tissues of the Ad-C and Ad-Brd2 mice. The adipose tissues were cut into pieces about 1 mm^2 size and incubated at 37 °C in Krebs Ringer buffer containing 2% fatty acid-free BSA for 1 h. Collected supernatant after a centrifugation at 3000 × *g* for 5 min and then assaying for glycerol content. Glycerol release was normalized to cellular protein content. Cells were planted into 96-well plates at a consistent density. Differentiated 3T3-L1 adipocytes were incubated in Phenol red–free DMEM and in the presence or absence of 100 nM insulin for the indicated time (0 h, 2 h, 4 h, 6 h). The supernatant was then collected, and cell fragments were removed by centrifugation at 4 °C, 12000 × *g* for 15 min.

The glycerol release was measured in 96-well plates using the free glycerol reagent kit (Sigma, St. Louis, MO).

2.8. Cell culture and induction of differentiation

Murine 3T3-L1 cells were cultured in DMEM containing 10% normal calf serum, 8 mg/ml biotin-calcium pantothenate, 100 IU/ml penicillin, and 100 IU/ml streptomycin. For adipocyte differentiation, fully confluent cells were cultured for 3 days in high-glucose DMEM containing 10% foetal bovine serum (FBS), 1 μM Dexamethasone (Dex), 0.5 mM 1-methyl-3-isobutyxanthine (Mix), and 1 μg/ml insulin. The cells were then cultured in post-differentiation medium containing 10% FBS and 5 μg/ml insulin. The medium was replaced 2 days later with high-glucose DMEM containing 10% FBS and was subsequently refreshed every other day. The cells were maintained at 37 °C in 5% CO_2. For our in vitro experiments, purified Ad-Brd2 or Ad-C were transfected into the 3T3-L1 cells on day 5 after differentiation was induced.

2.9. Palmitic acid (PA)-induced insulin resistance model

Briefly, 10 mM PA storage solution was prepared by adding PA to 0.1 M NaOH, clarifying it in 70 °C water, mixing it with the 10% BSA (FFA-free), and finally adjusting the pH to a neutral pH with HCl. The solution was added to medium at the appropriate concentration to induce the insulin resistance model after PA-stimulation for 16 h.

2.10. Western blot analysis

Cells or adipose tissue were washed twice with ice-cold PBS and solubilized in 2% sodium dodecyl sulfate (SDS) containing phosphatase and protease inhibitors for 30 min. Insoluble material was removed by centrifugation at 12000 × *g* for 15 min. The supernatant of each sample was collected and detected using the bicinchoninic acid (BCA) protein quantitative kit (Thermo Scientific, Waltham, MA, USA). The load volume of each sample was adjusted according to the sample concentration to ensure that each protein sample was 40 μg. The proteins were then separated by SDS-polyacrylamide gel electrophoresis and transferred to a polyvinylidene difluoride membrane (Millipore, Billerica, MA, USA). After the membrane was blocked at room temperature for 1 h with 5% non-fat dry milk in PBS containing 0.1% Tween-20, it was incubated with primary antibodies diluted in blocking buffer overnight at 4 °C. The membrane was then washed three times for 10 min each with Tris-buffered saline containing 0.1% Tween 20 and incubated with rabbit secondary antibodies for 1 h at room temperature. After additional washes, the antibody-bound proteins were detected using a chemiluminescent substrate (PI34077; Thermo Scientific, Waltham, MA, USA) and an image of the membrane was captured on a film (Bio-Rad, Hercules, CA, USA).

2.11. RNA extraction and quantitative Real-Time PCR (qPCR)

The WAT was collected and immediately frozen in liquid nitrogen. Thereafter, the tissue samples were individually pulverized in a Cryo-Cup grinder. Total RNA was extracted from 3T3-L1 adipocytes and the pulverized tissues samples using Trizol regent (Vazyme, NJ) according to the manufacturer's instructions. Total RNA was then purified using the RNeasy Mini Kit and RNase-free DNase I (Qiagen, Germany). The quality and concentration of total RNA were determined by spectrophotometry at 260 nm / 280 nm radio with NanoDrop 2000 (Thermo Fisher Scientific, USA).

Then, cDNA was synthesized in 20 μl reactions with 1 μg of total RNA as the template using the HiScript 1st Strand cDNA Synthesis Kit (Vazyme, NJ) following the manufacturer's instructions. Reactions were performed under the following conditions: first, 1 μg RNA, 4 μl 4 × DNA Wiper Mix, and RNase-free water (up to 16 μl) were mixed, and the reaction was incubated at 42 °C for 2 min to remove genomic DNA. Then, 4 μl HiScript III qRT SuperMix was added into the mix and incubated it at 37 °C for 15 min. Reactions were heat inactivated at 85 °C for 5 min. Finally the cDNA samples were stored at −20 °C until further use.

The sequences of qPCR primers are listed in Table 2. Primers for qPCR were designed with the Primer 3 software and verified with Primer-BLAST from the NCBI website. The amplification efficiency of primers was validated to be 95%-105% before use. qPCR reactions were performed using SYBR Green PCR Master Mix Kit (Vazyme, NJ), according to the manufacturer's protocol. Individual samples were run in triplicate in 20 μl reaction volumes containing 10 μl 2 × ChamQ Universal SYBR qPCR Master Mix, 0.4 μl of each primer (final concentration 10 μM), 2 μl diluted cDNA and 7.2 μl nuclease-free water using an ABI 7500 real-time PCR system (Applied Biosystems, CA). Reactions were run in 96-well plates under the following conditions: activation at 95 °C for 30 s, and 40 cycles of 95 °C for 10 s plus 60 °C for 30 s. A dissociation step consisting of 95 °C for 15 s, 60 °C for 1 min, 95 °C for 15 s and 60 °C for 15 s was performed at the end to ensure the specificity of PCR amplification. qPCR data were analysed using the ΔΔCT method with β-actin as the reference gene. Total RNA without reverse

Table 2
Primer sequences of various mouse genes were designed for qPCR. Primers were designed using Primer 3 software.

Gene	Accession No.	Size (bp)	Forward primer/Reverse primer (5′-3′)
Brd2	XM_017317246.1	141	GTTGCAGGATGTCAGTGGAC/GACGAGGAGCTGGAATCTGA
HSL	NM_010719.5	135	TGAGATGGTAACTGTGAGCC/ACTGAGATTGAGGTGCTGTC
ATGL	NM_025802.3	190	ACTGTGGCCTCATTCCTCCT/AACTGGATGCTGGTGTTGGT
SREBP-1	XM_006532716.2	165	TATGGAGGGCATGAAACCCGAAG/TTGACCTGGCTATCCTCAAAG
LDLR	NM_001252659.1	146	TCCACTGTGGTAGCAGTGAG/GTGAATGCAGGAGCCATCTG
FAS	XM_011247141.1	136	ACAAACTGCACCCTGACCCAGA/TGCTGGTTGCTGTGCATGGCT
Adiponectin	NM_009605.5	104	AGACCTGGCCACTTTCTCCTCATT/AGAGGAACAGGAGAGCTTGC
Perilipin 1	NM_001113471.1	171	CTGTGTGCAATGCCTATGAGA/CTGGAGGGTATTGAAGAGCCG
β-actin	NM_007393.5	285	TCATGAAGTGTGACGTTGACATC/CCTAGAAGCATTTGCGGTGCA

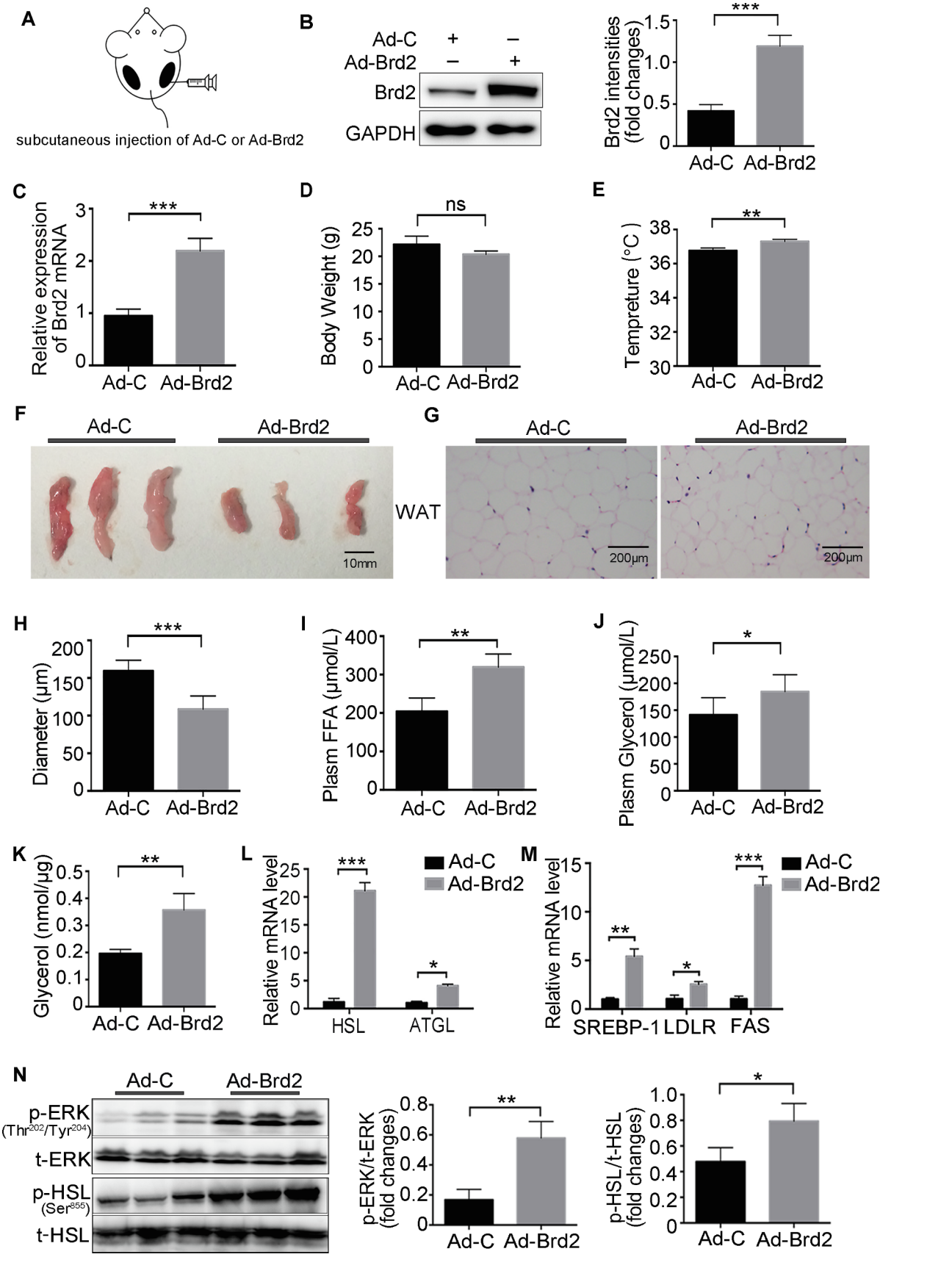

(caption on next page)

Fig. 1. Brd2 overexpression promotes lipolysis and FFA release in adipose tissues. (A) Recombinant adenovirus expressing Brd2 (Ad-Brd2) or LacZ (control, Ad-C) was subcutaneously injected into both sides of the inguinal fat pad in mice (n = 6 per group). Mice were injected twice a week with the purified adenovirus for 4 weeks. (B) Brd2 protein expression in WAT was analysed by western blotting and then quantified using image J software. (C) The relative mRNA expression of Brd2 was assessed by qPCR in WAT of mice. (D) Body weight, (E) temperature of Ad-C- and Ad-Brd2-treated mice. (F) Representative images of the subcutaneous fat isolated from male mice with or without Brd2 overexpression. (G) Representative images of haematoxylin and eosin-stained sections of the subcutaneous fat from male mice with or without Brd2 overexpression. (H) Morphometric analysis of adipocyte cell diameter in the haematoxylin-eosin-stained fat sections of Ad-C- and Ad-Brd2-treated mice. (I) Plasma FFA levels, (J) plasma glycerol levels for mice on a normal chow diet injected with Ad-C or Ad-Brd2. (K) Glycerol release from subcutaneous adipocyte tissues injected with Ad-C or Ad-Brd2. (L) qPCR detection of genes related to lipolysis or (M) fat synthesis in the WAT of mice in each group. (N) Western blotting analysis and quantitation of phosphorylated (p-)ERK, total (t-)ERK and (p-)HSL, (t-)HSL upon Ad-Brd2 or Ad-C injection in mice. Data are expressed as the mean ± SEM of at least three experiments and were analysed using one-way ANOVA. $*p < 0.05$, $**p < 0.01$, $***p < 0.001$, ns: not significant.

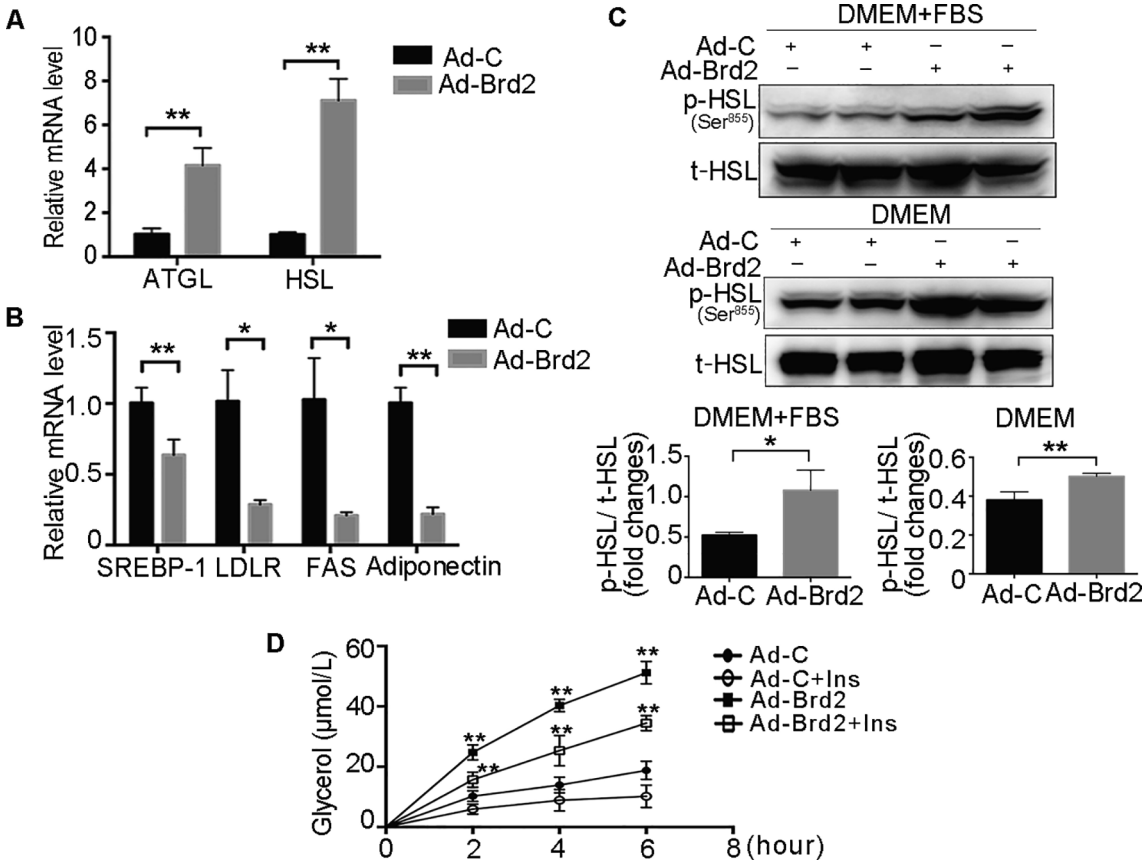

Fig. 2. Brd2 overexpression increases lipolysis in 3T3-L1 adipocytes. qPCR analysis of gene expression related to lipolysis (A) or fat synthesis (B) treated with Ad-C or Ad-Brd2 in 3T3-L1 adipocytes. (C) Western blotting analysis and quantitation of phosphorylated (p-)HSL and total (t-)HSL upon Ad-Brd2 or Ad-C infection in 3T3-L1 cells. In order to eliminate the interference of serum on ERK activity, cells were cultured under normal conditions (DMEM + FBS) or serum starvation conditions (DMEM). (D) A glycerol release test was performed on cells treated with Ad-C or Ad-Brd2 that were pre-treated with or without insulin (100 nM) for 0 h, 2 h, 4 h and 6 h. Data are expressed as the mean ± SEM of at least three experiments and were analysed using two-way ANOVA. $*p < 0.05$, $**p < 0.01$.

transcription was used as a negative control to check for contamination of genomic DNA, and water in place of cDNA was used to check for primer-dimer formation and reagent contamination. Relative quantities calculated as $2^{-\Delta\Delta CT}$ were used for statistical analysis.

2.12. Immunofluorescence analysis

3T3-L1 cells were transferred onto Matrigel-coated coverslips in culture plates. After the cells formed a monolayer, the coverslips were removed and washed twice with ice-cold PBS. The cells were then fixed with 4% paraformaldehyde for 20 min on ice and washed three times for 5 min each with PBS. After blocking with PBS containing 0.1% Triton X-100 and 1% bovine serum albumin for 30 min at room temperature, the samples were incubated overnight at 4 °C with primary antibodies, washed three times with PBS, and incubated at room temperature for 1 h with goat anti-rabbit Alexa Fluor 555 antibodies (Abcam, Cambridge, MA, USA) in blocking buffer. Next, the cells were treated with ProLong Gold antifade reagent containing 4′, 6-diamidino-2-phenylindole (Invitrogen), washed three times with PBS, and mounted. The cells were examined using a confocal laser scanning microscope (Leica, Wetzlar, Germany).

2.13. Statistical analysis

Data represent the mean ± standard error of the mean. Groups were compared by one-way analysis of variance followed by an unpaired two-tailed Student's *t*-test using Prism v.6.0b software for Mac (GraphPad Inc., San Diego, CA, USA). Differences were considered statistically significant at $p < 0.05$.

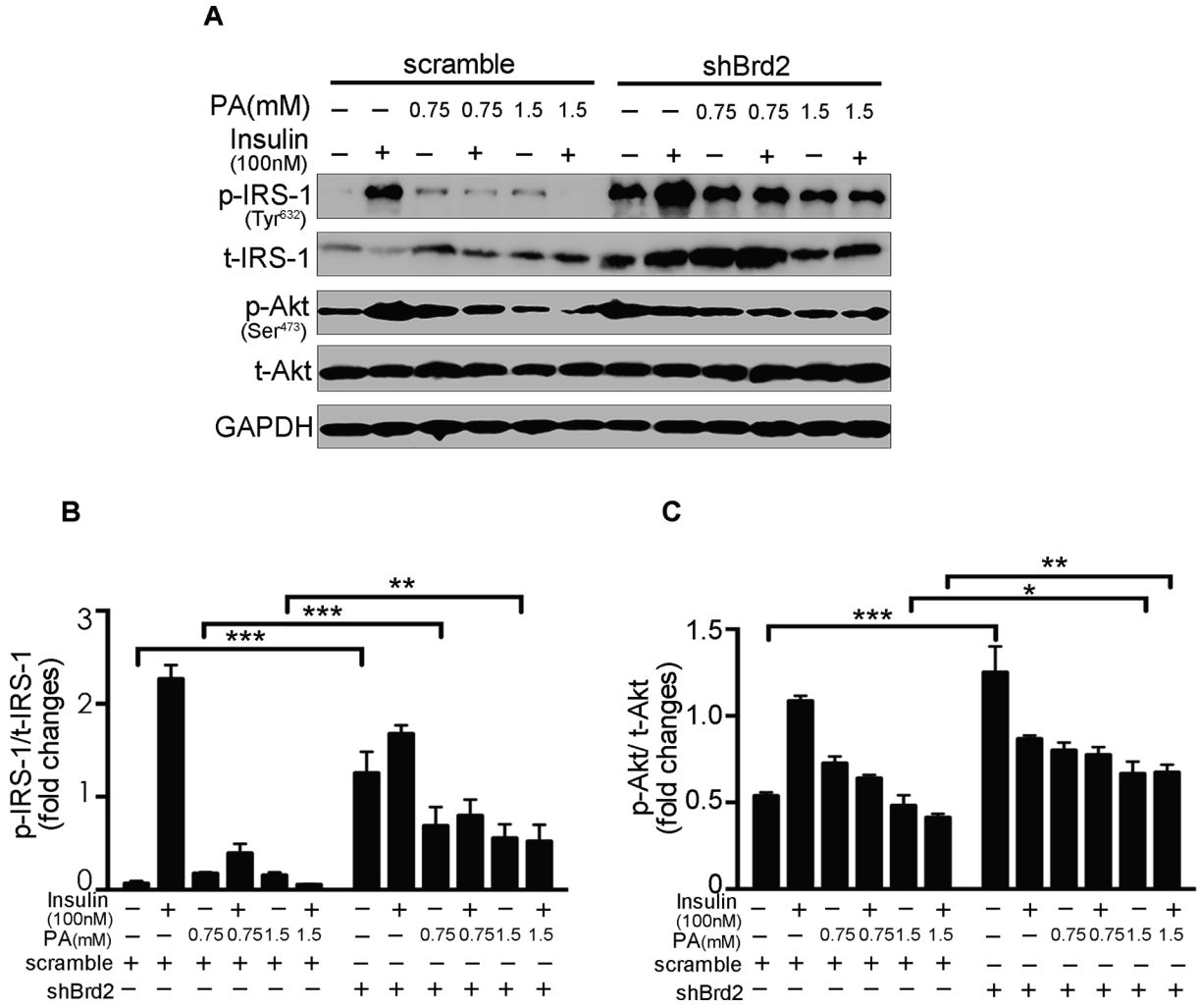

Fig. 3. Downregulation of Brd2 improves insulin resistance related signalling pathways. (A-C) shBrd2 group: using the shRNA targeting mouse Brd2 to knockdown Brd2 expression. scramble group: using scrambled shRNA as the control. 3 T3-L1 adipocytes were transfected with shBrd2 or scramble on day 5 after adipogenic induction. Cells were harvested after treatment with 0 mM, 0.75 mM, and 1.5 mM palmitic acid for 16 h, followed by addition of 100 nM insulin for 5 min. Western blotting analysis and quantitation of phosphorylated (p)-IRS-1, total (t)-IRS-1, p-Akt, t-Akt, and GAPDH. Data are expressed as the mean ± SEM of at least three experiments and were analysed using one-way ANOVA. $*p < 0.05$, $**p < 0.01$, $***p < 0.001$.

3. Results

3.1. Brd2 overexpression alleviates fat deposition in WAT and facilitates lipolysis in mice

To investigate the role of Brd2 in lipid metabolism in vivo, recombinant Ad-Brd2 was subcutaneously injected into the area beside the inguinal fat pad in mice (Fig. 1A). This resulted in Brd2 overexpression in WAT (Fig. 1B and C). While there were no differences in body weight among the groups (Fig. 1D), body temperature was markedly increased in Ad-Brd2-treated mice compared with control mice (Fig. 1E). Furthermore, the WAT deposits in Brd2 overexpression group were smaller than those observed in the controls (Fig. 1F). Interestingly, haematoxylin and eosin staining also revealed that the diameter of fat cells in the WAT of mice overexpressing Brd2 was smaller than that in the WAT of control mice (Fig. 1G and H). Compared with levels in the control group, plasma FFA or plasma glycerol levels in Ad-Brd2-treated mice were increased significantly (Fig. 1I and J). We next tested glycerol release from subcutaneous white adipocyte tissues, and the results also showed that overexpression of Brd2 increased glycerol release (Fig. 1K), indicating that Brd2 overexpression increased WAT lipolysis.

Next, we analysed the expression of lipolysis-related genes in mice, including HSL and ATGL, to further explore the regulatory role of Brd2 on lipolysis. Our results show that the mRNA expression of these genes was upregulated by Brd2 overexpression (Fig. 1L), with that of HSL being almost 10 times higher than that of the control group. Surprisingly, genes related to fat synthesis, including sterol regulatory element-binding proteins 1 (SREBP-1), low-density lipoprotein receptor (LDLR), and fatty acid synthase (FAS) (Galles et al., 2018), were also upregulated in Brd2-overexpressing mice (Fig. 1M), suggesting that Brd2-mediated activation of lipolysis-related genes might trigger a negative feedback loop to promote fat synthesis. It has been reported that the ERK signalling pathway could stimulate lipolysis by activating HSL phosphorylation level (Larsson et al., 2016). We found that overexpression of Brd2 in mice significantly increased the phosphorylation of ERK and HSL to activate the ERK signalling pathway (Fig. 1N). Thus, Brd2 overexpression in adipose tissue appears to activate lipolysis, resulting in excessive FFA release in vivo.

3.2. Effects of Brd2 overexpression on lipolysis in 3T3-L1 adipocytes

Based on our observation that Brd2 promoted lipolysis in vivo, we tested whether the same effect occurred in vitro. Notably, the expression of lipid metabolism-related genes, including ATGL and HSL, appeared to be strongly induced in vitro, with the Brd2-overexpressing

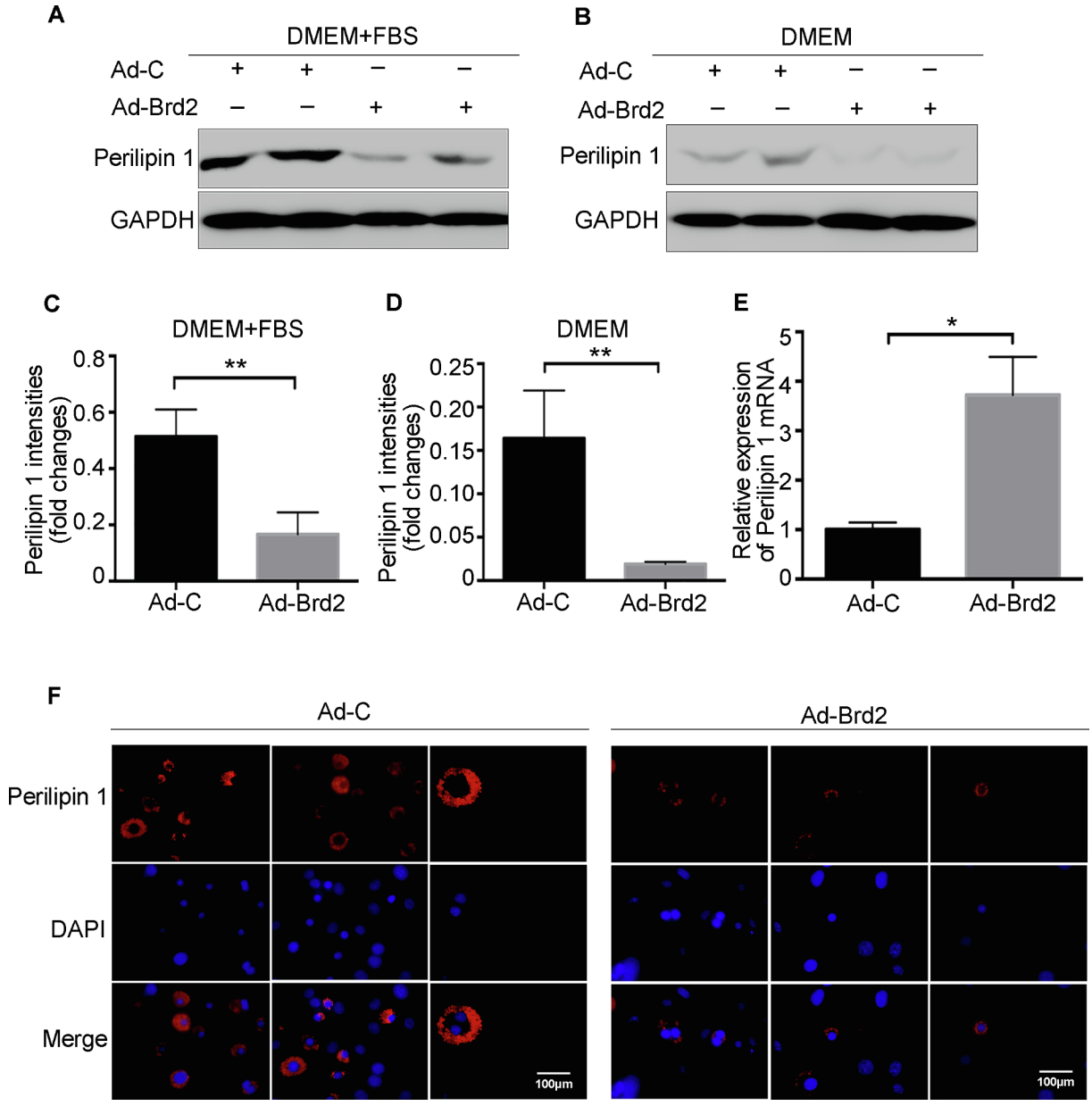

Fig. 4. Brd2 reduces perilipin 1 expression in 3T3-L1 adipocytes. (A-D) Western blotting analysis and quantitation of perilipin 1 3T3-L1 adipocytes overexpressing Brd2 with FBS treatment in serum (DMEM + FBS) or serum starved conditions (DMEM). (E) the relative mRNA expression of perilipin 1 was detected by qPCR in 3T3-L1 adipocytes infected with Ad-C or Ad-Brd2. (F) Perilipin 1 immunofluorescence (red) in 3T3-L1 pre-adipocytes treated with Ad-C or Ad-Brd2. Data are expressed as the mean ± SEM of at least three experiments and were analysed using one-way ANOVA. $^{*}p < 0.05$, $^{**}p < 0.01$. Scale bars: 100 μm.

mature adipocytes expressing much higher levels than the control cells (Fig. 2A). In contrast to our in vivo findings, Brd2 overexpression in 3T3-L1 adipocytes reduced the levels of the fat synthesis-related genes SREBP-1, LDLR, FAS, and adiponectin (Fig. 2B). Brd2 overexpression also promoted HSL phosphorylation at Ser855 (Fig. 2C), a phenomenon that appeared to be potentiated by serum starvation (Fig. 2C). These data indicate that Brd2 likely functions in lipolysis via HSL activation.

Insulin plays an important role in lipid metabolism. Short-term stimulation with insulin can effectively inhibit lipolysis and promote fat synthesis (Pal et al., 2012). Thus, to test the effect of Brd2 on glycerol release during lipolysis, we measured glycerol levels in 3T3-L1 adipocytes with insulin stimulation at 0 h, 2 h, 4 h and 6 h in the Ad-Brd2 and Ad-C groups. As shown in Fig. 2D, Brd2 overexpression partially attenuates the inhibitory effect of insulin on lipolysis, thereby facilitating glycerol release. Taken together, these results indicate that Brd2 enhances lipolysis both in vivo and in vitro.

It has been reported that treatment with palmitic acid could be used as an insulin resistance model in adipocytes (Wang et al., 2010). Next, we verified whether Brd2 was associated with FFA-induced insulin resistance. 3T3-L1 adipocytes were transfected with shRNA vectors against Brd2 (shBrd2) to knockdown Brd2 expression, using the scrambled shRNA (scramble) as the control group. After adding different concentrations of palmitic acid to the medium, the phosphorylation levels of IRS-1 and Akt were inhibited to some extent (Fig. 3A). However, compared with the control group, the phosphorylation of IRS-1 and Akt were increased significantly in Brd2 downregulated group, especially in the high concentration with palmitic acid treatment (Fig. 3B and C), Thus, these results demonstrate that the inhibition of palmitic acid on the insulin signalling pathway can be significantly reduced by Brd2 downregulation, thereby improving the insulin sensitivity.

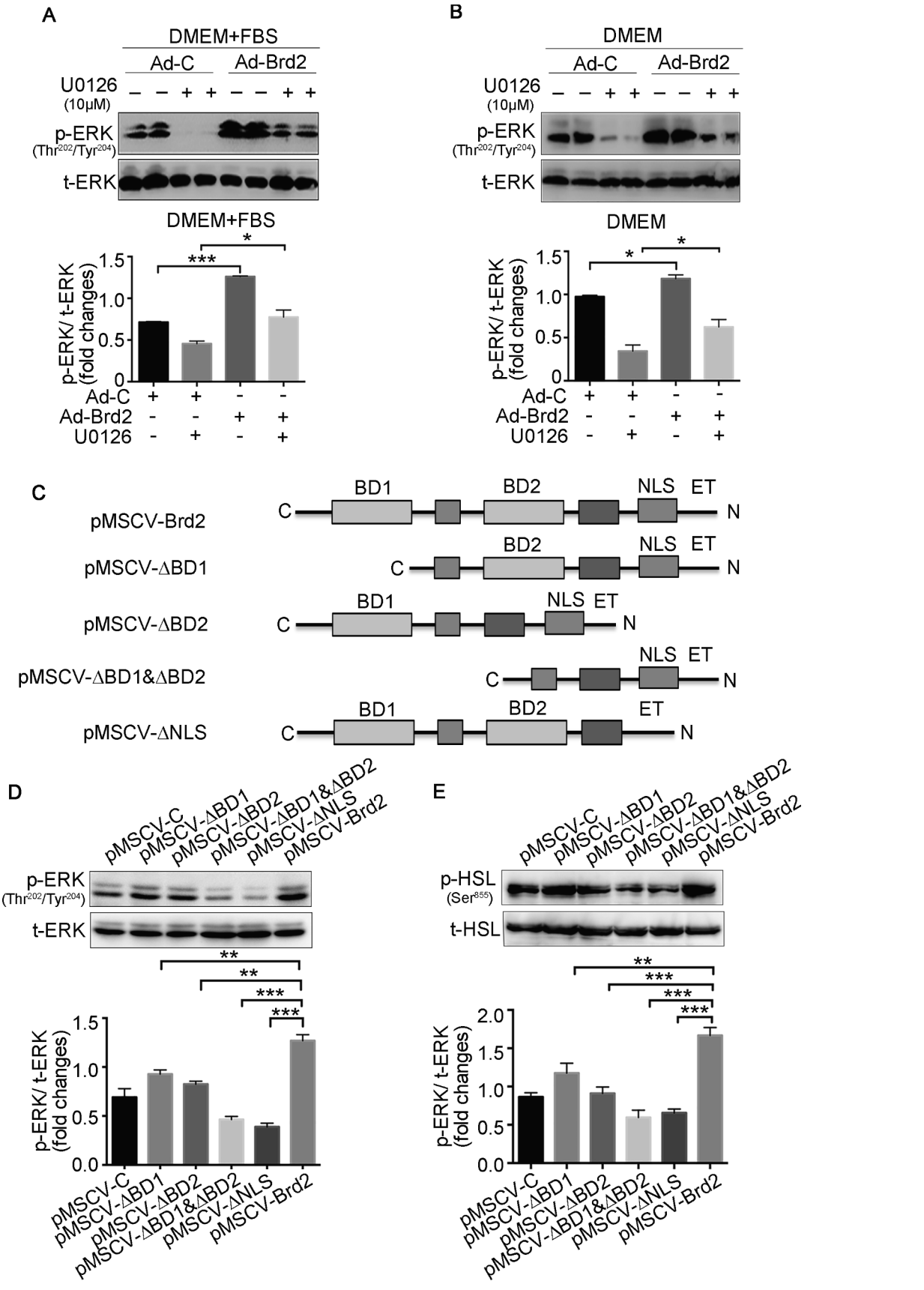

(caption on next page)

Fig. 5. Brd2 overexpression activates ERK phosphorylation. (A, B) Western blotting analysis and quantitation of phosphorylated (p-)ERK and total (t-)ERK expression in Ad-C- and Ad-Brd2- treated 3T3-L1 cells with or without U0126 (the MAPK inhibitor) treatment in serum (DMEM + FBS) or serum starved conditions (DMEM). (C) Construction of four Brd2 domain deletion mutations, including ΔBD1, ΔBD2, ΔBD1&ΔBD2, ΔNLS and overexpression plasmid (pMSCV-Brd2). (D) Western blotting analysis and quantitation of phosphorylated (p-)ERK, total (t-)ERK and (p-)HSL, total (t-)HSL expression with the treatment of overexpressing wild type, ΔBD1, ΔBD2, ΔBD1&ΔBD2, ΔNLS, pMSCV-Brd2. Data are expressed as the mean ± SEM of at least three experiments and were analysed using one-way ANOVA. $^{*}p < 0.05$, $^{**}p < 0.01$, $^{***}p < 0.001$.

3.3. Brd2 promotes perilipin 1 degradation in 3 T3-L1 adipocytes

Perilipin 1, a lipid droplet-associated protein found in adipocytes and steroidogenic cells, plays a crucial role in lipolysis regulation (Londos et al., 1999; Zhang et al., 2018a,b). We further tested whether Brd2 regulated lipolysis was related to perilipin 1. As shown in Fig. 4A–D, Brd2 overexpression decreased perilipin 1 protein expression (Fig. 4A–D). Interestingly, qPCR analysis showed that overexpressing Brd2 increased perilipin 1 expression (Fig. 4E), indicating that regulation likely occurs at the protein level rather than the transcriptional level (Brasaemle et al., 1997). Immunofluorescence analysis was also used to confirm that Brd2 overexpression promoted perilipin 1 protein degradation relative to the control group (Fig. 4F). Thus, Brd2 also appears to facilitate lipolysis, at least partly, by inducing perilipin 1 degradation.

3.4. Activation of ERK is related to Brd2 histone acetylation

The ERK pathway has been known to participate in lipolysis and is related to changes in perilipin 1 expression (Drira and Sakamoto, 2014; Larsson et al., 2016; Wu et al., 2018). To clarify the effects of Brd2 overexpression on this signalling cascade, we examined ERK expression by western blotting. Our data showed that ERK phosphorylation was increased following Brd2 overexpression compared to the control group (Fig. 5A and B). Additionally, U0126, an inhibitor of mitogen-activated protein kinases (MAPK) pathway, can inhibit the phosphorylation of ERK and then reducing HSL activity (Greenberg et al., 2001). After treatment with U0126, ERK phosphorylation was significantly inhibited, but Brd2 overexpression partly restored ERK activity in treated adipocytes (Fig. 5A and B). To further clarify the regulatory mechanism of Brd2 on ERK, we constructed four protein domain mutant plasmids, respectively (Fig. 5C). Compared with the Brd2 overexpressing group and the wild type group, we found that both the BD1 and BD2 domains had regulatory effects on promoting lipolysis, which increased ERK and HSL phosphorylation levels (Fig. 5D and E). However, when either nuclear location signal (NLS) or BD (BD1 and BD2) domains was deleted, phosphorylation of ERK and HSL were significantly reduced (Fig. 5D and E). A previous study reported that both the BD1 and BD2 domains contained histone acetylation binding sites (Sinha et al., 2005). Therefore, we speculate that ERK phosphorylation may be associated with transcriptional regulation of Brd2 through histone acetylation.

3.5. Brd2 regulates lipid metabolism through the ERK/HSL pathway

Furthermore, we found that Brd2 overexpression could increase the U0126-inhibited HSL expression (Fig. 6A). However, the same effect was not observed for the U0126-mediated inhibition of ATGL (Fig. 6B). Western blotting analysis also showed that HSL phosphorylation was increased by Brd2 overexpression relative to the control group (Fig. 6C and D). This increase in HSL phosphorylation was also accompanied by a decrease in perilipin 1 protein expression (Fig. 6C and D). Moreover, while treatment with U0126 reduced HSL phosphorylation and partly restored perilipin 1 activity, Brd2 overexpression diminished these effects (Fig. 6C and D). Next, we performed a glycerol release assay, which demonstrated that Brd2 overexpression stimulated glycerol release and reduced the inhibitory effects of U0126 on this process (Fig. 6E and F). Therefore, these results cumulatively indicate that Brd2 likely induces HSL hydrolysis via ERK signalling, thereby suppressing perilipin 1 expression and, ultimately, promoting lipolysis and inducing insulin resistance.

4. Discussion

Accumulating genetic evidence indicates that both abnormal FFA metabolism and inactivation of insulin signalling pathways can lead to insulin resistance (Fernandes et al., 2012; Roden, 2006; Zabielski et al., 2018), but the specific regulatory mechanism is unclear.

Several factors cause adipose tissue metabolism abnormalities, such as FFA re-esterification as well as de novo synthesis (Acosta et al., 2016; Pereira et al., 2016). However, recent studies have showed that people with T2DM are also accompanied by abnormal lipolysis in adipose tissue (Ivanov et al., 2014; Kahl et al., 2014; Morigny et al., 2016), which may lead to increased accumulation of FFA in plasma. A previous study demonstrated that *Brd2* knockout mice developed obesity but not insulin resistance or T2DM (Wang et al., 2009); however, insulin resistance was showed to be increased in mice overexpressing Brd2 (Sun et al., 2017). Unfortunately, the molecular mechanisms of these Brd2-induced changes are largely unknown. In this study, we evaluated the effects of Brd2 overexpression in vivo and in vitro to elucidate the signalling pathways involved in lipolysis. Moreover, downregulation of Brd2 could improve insulin resistance induced by palmitic acid (Fig. 3), indicating that insulin resistance caused by Brd2 may be related to the accumulation of FFA and FFA metabolites. The results of our study demonstrate that Brd2 overexpression dysregulates lipid metabolism, resulting in inappropriate FFA release and insulin resistance.

In our Brd2-overexpressing mouse model, we observed Brd2 overexpression-mediated changes in the expression of lipolysis-related genes ATGL and HSL. However, the mRNA levels of the fat synthesis-related enzymes SREBP-1, LDLR, and FAS in vivo were concomitantly increased, which was inconsistence with that in 3T3-L1 adipocytes. We speculate that the environment in vivo is relatively complex, and it is possible that Ad-Brd2 can significantly promote lipolysis to induce a negative feedback regulation in mice, thereby promoting the expression of the genes associated with fat synthesis to maintain metabolic homeostasis (Figs. 1M and 2B). Obviously, overexpression of Brd2 promoted lipolysis-related activity of ERK/HSL signalling pathway in mice (Fig. 1N). In addition, we found that the body temperature of mice overexpressing Brd2 increased. This change was accompanied by a marked decrease in WAT size relative to the control group (Fig. 1E–H). These data imply that Brd2 overexpression results in an abnormal increase in lipolysis, leading to FFA release. However, studies have also shown that the browning of WAT can promote heat generation in the body, thereby increasing the basal body temperature (Reverte-Salisa et al., 2018; Sepa-Kishi and Ceddia, 2018; Zhang et al., 2018a,b). Therefore, in future studies, we will clarify the regulatory mechanism of Brd2 in white fat browning.

In 3T3-L1 adipocytes, Brd2 overexpression stimulated HSL and ATGL mRNA expression and suppressed that of SREBP-1, LDLR, and FAS, resulting in enhanced glycerol release (Fig. 2). Moreover, adiponectin, which increases insulin activity in the liver and/or muscle (Yadav et al., 2013), was significantly inhibited by Brd2 overexpression. Thus, Brd2 appears to restrain adipocytokines secretion and induce insulin resistance. Furthermore, we observed that Brd2 overexpression increased HSL phosphorylation and decreased perilipin 1 protein expression (Figs. 2C and 4). Previous studies have shown that

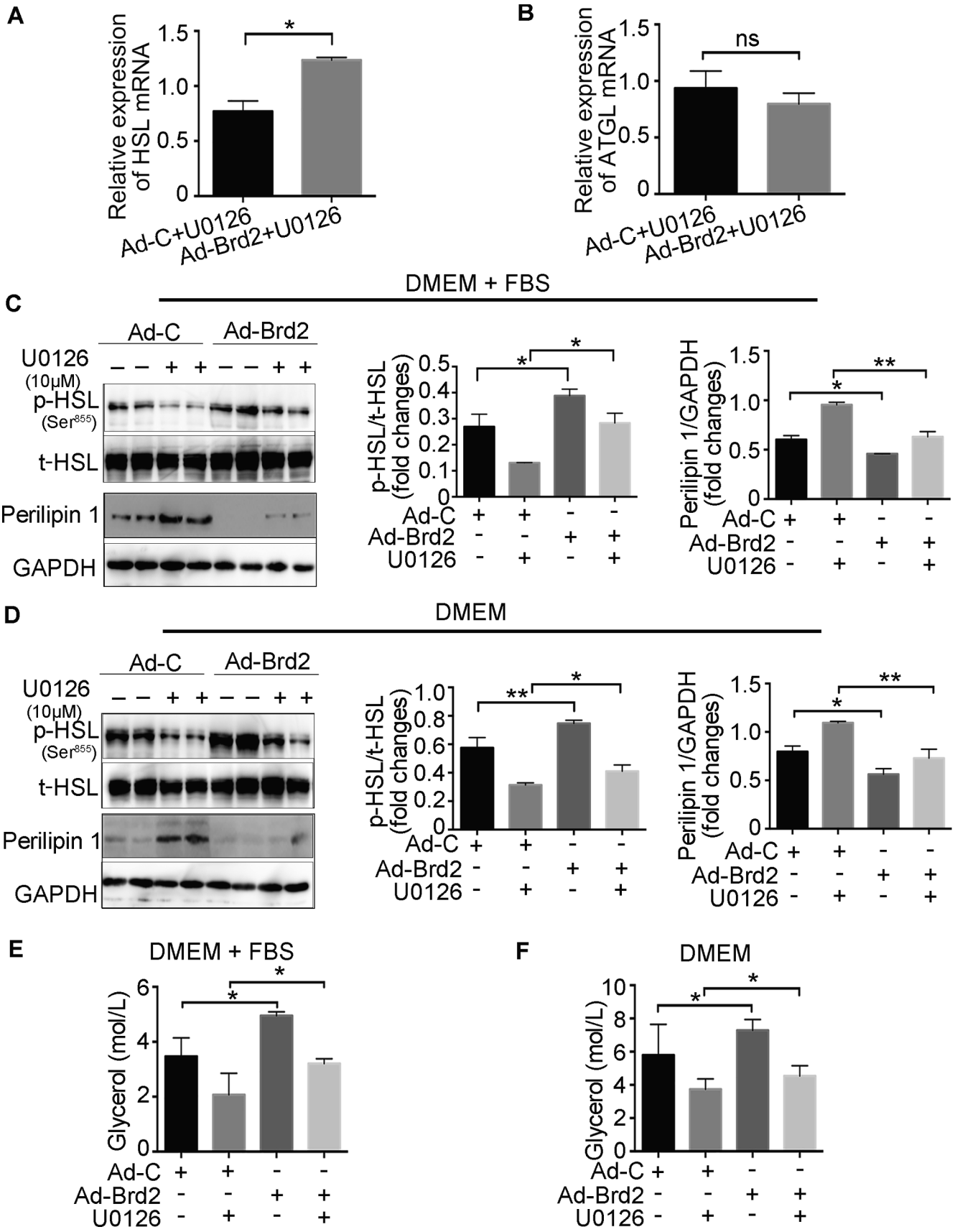

Fig. 6. Brd2 overexpression activates ERK/HSL signalling pathway. qPCR analysis of HSL (A) and ATGL (B) in Ad-C- and Ad-Brd2- treated 3T3-L1 cells with U0126 treatment. (C, D) Western blotting analysis and quantitation of phosphorylated (p-)HSL and total (t-)HSL as well as perilipin 1 in Ad-C- and Ad-Brd2- treated 3T3-L1 cells with or without U0126 treatment in serum (DMEM + FBS) or serum starved conditions (DMEM). (E, F) A glycerol release test was performed on 3T3-L1 adipocytes infected with Ad-Brd2 with or without 10 μM U0126 treatment in serum (DMEM + FBS) or serum starved conditions (DMEM). Data are expressed as the mean ± SEM of at least three experiments and were analysed using one-way ANOVA. *$p < 0.05$, **$p < 0.01$, ns: not significant.

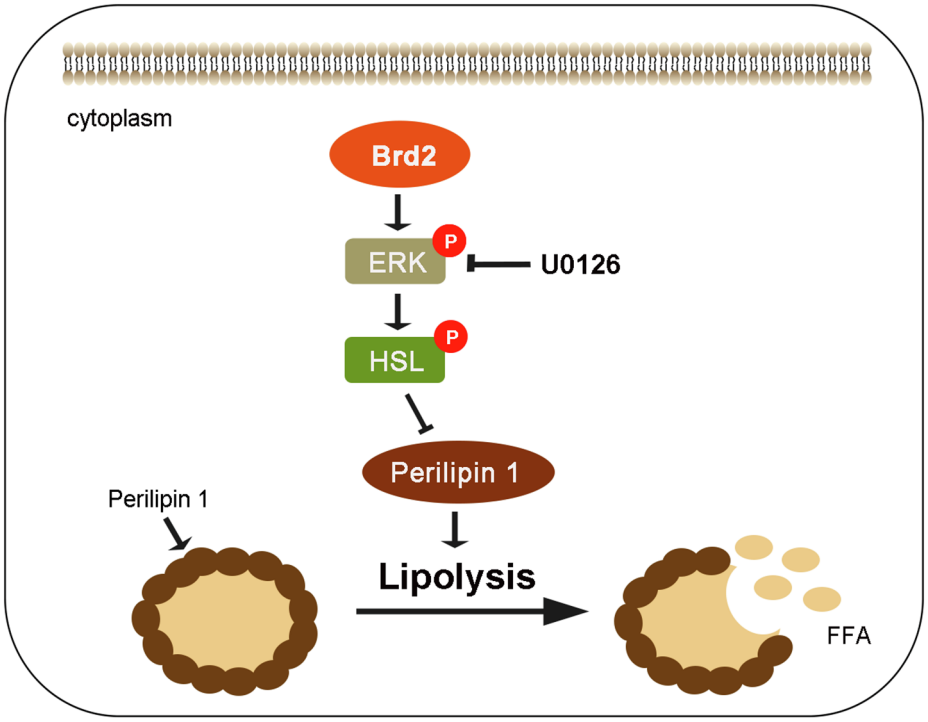

Fig. 7. Schematic model for Brd2 regulation of lipolysis through the ERK/HSL signalling pathway.

perilipin 1 is mainly distributed in lipid droplets and mostly regulated post-translationally (Brasaemle et al., 1997; Londos et al., 1999), which may explain the observed discrepancy between perilipin 1 mRNA and protein expression after Brd2 treatment (Fig. 4). Under normal conditions, non-phosphorylated perilipin 1 forms a barrier on the lipid droplet surface that prevents lipase from degrading the triglycerides, thereby limiting lipolysis (Londos et al., 1999; Londos et al., 2005). Downregulation and/or phosphorylation of perilipin 1 will, therefore, allow lipase to contact and degrade the triglycerides in the droplet, unsettling lipid metabolism homeostasis (Zhang et al., 2018a,b).

Most of the signalling pathways involved in lipolysis are related to HSL phosphorylation (Prentki et al., 2013). However, degradation of perilipin 1 is associated with the ERK signalling pathway (Larsson et al., 2016). Using the MAPK inhibitor, U0126, we found that Brd2 overexpression restored the U0126-depleted activity of HSL, but these effects were not observed for ATGL (Fig. 6A–B). However, the mRNA and protein levels of HSL were inconsistent (Fig. 6A, C and Fig. 2A, C), which may be due to the fact that expression of HSL protein is partly determined by mRNA, and Brd2 overexpression mainly have affected its post-transcriptional regulation and phosphorylation (Large et al., 1998). These results suggest that Brd2 overexpression mainly regulates lipolysis through the ERK/HSL pathway. Indeed, we observed that Brd2 activated the ERK signalling pathway via ERK kinase phosphorylation and then promoted HSL phosphorylation level, which is related to the function of the BD1 and BD2 bromodomain functional domains (Fig. 5). As shown in Fig. 5, deletion of either BD1 or BD2 also promoted the phosphorylation of ERK compared with Brd2 overexpression and the wild type, but deletion of both BD1 and BD2 inhibited ERK activation, indicating that both the BD1 and BD2 domains may be involved in the regulation of ERK phosphorylation to promote lipolysis. We previously showed that Brd2 promotes the release of tumour necrosis factor-α (TNF-α) and interleukin-6 (IL-6) by affecting nuclear factor-κB-mediated inflammation (Sun et al., 2017), and a related research showed that TNF-α and IL-6 subsequently activated ERK sequentially (Bezaire et al., 2009a,b; Yang and Yang, 2010). Moreover, when the Brd2 nuclear localization signal was deleted, the activation of ERK phosphorylation was blocked, suggesting that this process may be related to the regulation of histone acetylation in the nucleus by Brd2 (Fig. 5C-E). Some studies have reported that the expression of genes such as G protein-coupled receptors (GPCRs), tumour progression locus 2 (TPL2), and PKC in adipocytes was related to ERK phosphorylation and that these genes were also regulated by histone acetylation (Chorzalska et al., 2018; Kumari et al., 2016; Zhu et al., 2018). In future studies, we will continue to explore whether Brd2 is involved in regulating the acetylation of these genes, thereby affecting the activity of ERK.

In conclusion, we demonstrated that Brd2 could promote lipolysis by activating the ERK signalling pathway and stimulating HSL phosphorylation. These changes subsequently suppressed perilipin 1 expression and promoted FFA release into the plasma, resulting in insulin resistance (Fig. 7). Thus, targeted Brd2 inhibition (for instance, with JQ1) is a potential therapeutic approach for restoring normal lipid metabolism and preventing insulin resistance that can lead to T2DM. While future work will focus on the application of these findings, this study provides insight into the development of insulin resistance and T2DM pathogenesis.

Declaration of Competing Interest

The authors declare no conflict of interest.

Acknowledgements

This work was supported by Grants from the National Natural Science Foundation of China (No. 31671228), Shanghai Sailing Program (18YF1422000) and the National Key Research Project Biosafety Key Technology Development Program (2016YFC1201501).

Appendix A. Supplementary data

Supplementary data to this article can be found online at https://doi.org/10.1016/j.ygcen.2019.05.011.

References

Acosta, J.R., Douagi, I., Andersson, D.P., Backdahl, J., Ryden, M., Arner, P., Laurencikiene, J., 2016. Increased fat cell size: a major phenotype of subcutaneous white adipose tissue in non-obese individuals with type 2 diabetes. Diabetologia 59, 560–570.

Bartz, R., Zehmer, J.K., Zhu, M., Chen, Y., Serrero, G., Zhao, Y., Liu, P., 2007. Dynamic activity of lipid droplets: protein phosphorylation and GTP-mediated protein translocation. J. Proteome Res. 6, 3256–3265.

Belkina, A.C., Nikolajczyk, B.S., Denis, G.V., 2013. BET protein function is required for inflammation: Brd2 genetic disruption and BET inhibitor JQ1 impair mouse macrophage inflammatory responses. J. Immunol. 190, 3670–3678.

Bezaire, V., Mairal, A., Anesia, R., Lefort, C., Langin, D., 2009a. Chronic TNFalpha and cAMP pre-treatment of human adipocytes alter HSL, ATGL and perilipin to regulate basal and stimulated lipolysis. FEBS Lett. 583, 3045–3049.

Bezaire, V., Mairal, A., Ribet, C., Lefort, C., Girousse, A., Jocken, J., Laurencikiene, J., Anesia, R., Rodriguez, A.M., Ryden, M., Stenson, B.M., Dani, C., Ailhaud, G., Arner, P., Langin, D., 2009b. Contribution of adipose triglyceride lipase and hormone-sensitive lipase to lipolysis in hMADS adipocytes. J. Biol. Chem. 284, 18282–18291.

Brasaemle, D.L., Barber, T., Kimmel, A.R., Londos, C., 1997. Post-translational regulation of perilipin expression. Stabilization by stored intracellular neutral lipids. J. Biol. Chem. 272, 9378–9387.

Chorzalska, A., Ahsan, N., Rao, R.S.P., Roder, K., Yu, X., Morgan, J., Tepper, A., Hines, S., Zhang, P., Treaba, D.O., Zhao, T.C., Olszewski, A.J., Reagan, J.L., Liang, O., Gruppuso, P.A., Dubielecka, P.M., 2018. Overexpression of Tpl2 is linked to imatinib resistance and activation of MEK-ERK and NF-kappaB pathways in a model of chronic myeloid leukemia. Mol. Oncol. 12, 630–647.

Drira, R., Sakamoto, K., 2014. Hydroxytyrosol stimulates lipolysis via A-kinase and extracellular signal-regulated kinase activation in 3T3-L1 adipocytes. Eur. J. Nutr. 53, 743–750.

Fernandes, J., Vogt, J., Wolever, T.M., 2012. Intravenous acetate elicits a greater free fatty acid rebound in normal than hyperinsulinaemic humans. Eur. J. Clin. Nutr. 66, 1029–1034.

Fricke, K., Heitland, A., Maronde, E., 2004. Cooperative activation of lipolysis by protein kinase A and protein kinase C pathways in 3T3-L1 adipocytes. Endocrinology 145, 4940–4947.

Fruci, B., Giuliano, S., Mazza, A., Malaguarnera, R., Belfiore, A., 2013. Nonalcoholic Fatty liver: a possible new target for type 2 diabetes prevention and treatment. Int. J. Mol. Sci. 14, 22933–22966.

Galles, C., Prez, G.M., Penkov, S., Boland, S., Porta, E.O.J., Altabe, S.G., Labadie, G.R., Schmidt, U., Knolker, H.J., Kurzchalia, T.V., de Mendoza, D., 2018. Endocannabinoids in Caenorhabditis elegans are essential for the mobilization of cholesterol from internal reserves. Sci. Rep. 8, 6398.

Greenberg, A.S., Obin, M.S., 2006. Obesity and the role of adipose tissue in inflammation and metabolism. Am. J. Clin. Nutr. 83, 461S–465S.

Greenberg, A.S., Shen, W.J., Muliro, K., Patel, S., Souza, S.C., Roth, R.A., Kraemer, F.B., 2001. Stimulation of lipolysis and hormone-sensitive lipase via the extracellular signal-regulated kinase pathway. J. Biol. Chem. 276, 45456–45461.

Hong, S., Song, W., Zushin, P.H., Liu, B., Jedrychowski, M.P., Mina, A.I., Deng, Z., Cabarkapa, D., Hall, J.A., Palmer, C.J., Aliakbarian, H., Szpyt, J., Gygi, S.P., Tavakkoli, A., Lynch, L., Perrimon, N., Banks, A.S., 2018. Phosphorylation of Beta-3 adrenergic receptor at serine 247 by ERK MAP kinase drives lipolysis in obese adipocytes. Mol Metab. 12, 25–38.

Ivanov, V.V., Shakhristova, E.V., Stepovaya, E.A., Nosareva, O.L., Fedorova, T.S., Novitsky, V.V., 2014. Molecular mechanisms of modulation of lipolysis in adipose tissue and development of insulinresistance in diabetes. Patol. Fiziol. Eksp. Ter. 111–119.

Jaworski, K., Sarkadi-Nagy, E., Duncan, R.E., Ahmadian, M., Sul, H.S., 2007. Regulation of triglyceride metabolism. IV. Hormonal regulation of lipolysis in adipose tissue. Am. J. Physiol. Gastrointest. Liver Physiol. 293, G1–G4.

Johnson, G.L., Lapadat, R., 2002. Mitogen-activated protein kinase pathways mediated by ERK, JNK, and p38 protein kinases. Science 298, 1911–1912.

Kahl, S., Nowotny, B., Piepel, S., Nowotny, P.J., Strassburger, K., Herder, C., Pacini, G., Roden, M., 2014. Estimates of insulin sensitivity from the intravenous-glucose-modified-clamp test depend on suppression of lipolysis in type 2 diabetes: a randomised controlled trial. Diabetologia 57, 2094–2102.

Kahn, S.E., Hull, R.L., Utzschneider, K.M., 2006. Mechanisms linking obesity to insulin resistance and type 2 diabetes. Nature 444, 840–846.

Karpe, F., Dickmann, J.R., Frayn, K.N., 2011. Fatty acids, obesity, and insulin resistance: time for a reevaluation. Diabetes 60, 2441–2449.

Kumari, P., Srivastava, A., Banerjee, R., Ghosh, E., Gupta, P., Ranjan, R., Chen, X., Gupta, B., Gupta, C., Jaiman, D., Shukla, A.K., 2016. Functional competence of a partially engaged GPCR-beta-arrestin complex. Nat. Commun. 7, 13416.

Large, V., Arner, P., Reynisdottir, S., Grober, J., Van Harmelen, V., Holm, C., Langin, D., 1998. Hormone-sensitive lipase expression and activity in relation to lipolysis in human fat cells. J. Lipid Res. 39, 1688–1695.

Larsson, S., Jones, H.A., Goransson, O., Degerman, E., Holm, C., 2016. Parathyroid hormone induces adipocyte lipolysis via PKA-mediated phosphorylation of hormone-sensitive lipase. Cell. Signal. 28, 204–213.

Liu, F., Prabhakar, M., Ju, J., Long, H., Zhou, H.W., 2017. Effect of inulin-type fructans on blood lipid profile and glucose level: a systematic review and meta-analysis of randomized controlled trials. Eur. J. Clin. Nutr. 71, 9–20.

Londos, C., Brasaemle, D.L., Schultz, C.J., Adler-Wailes, D.C., Levin, D.M., Kimmel, A.R., Rondinone, C.M., 1999. On the control of lipolysis in adipocytes. Ann. N. Y. Acad. Sci. 892, 155–168.

Londos, C., Sztalryd, C., Tansey, J.T., Kimmel, A.R., 2005. Role of PAT proteins in lipid metabolism. Biochimie 87, 45–49.

Morigny, P., Houssier, M., Mouisel, E., Langin, D., 2016. Adipocyte lipolysis and insulin resistance. Biochimie 125, 259–266.

Pal, D., Dasgupta, S., Kundu, R., Maitra, S., Das, G., Mukhopadhyay, S., Ray, S., Majumdar, S.S., Bhattacharya, S., 2012. Fetuin-A acts as an endogenous ligand of TLR4 to promote lipid-induced insulin resistance. Nat. Med. 18, 1279–1285.

Peng, J., Dong, W., Chen, L., Zou, T., Qi, Y., Liu, Y., 2007. Brd2 is a TBP-associated protein and recruits TBP into E2F–1 transcriptional complex in response to serum stimulation. Mol. Cell. Biochem. 294, 45–54.

Pereira, M.J., Skrtic, S., Katsogiannos, P., Abrahamsson, N., Sidibeh, C.O., Dahgam, S., Mansson, M., Riserus, U., Kullberg, J., Eriksson, J.W., 2016. Impaired adipose tissue lipid storage, but not altered lipolysis, contributes to elevated levels of NEFA in type 2 diabetes. Degree of hyperglycemia and adiposity are important factors. Metabolism 65, 1768–1780.

Petersen, M.C., Vatner, D.F., Shulman, G.I., 2017. Regulation of hepatic glucose metabolism in health and disease. Nat. Rev. Endocrinol. 13, 572–587.

Pinent, M., Prokesch, A., Hackl, H., Voshol, P.J., Klatzer, A., Walenta, E., Panzenboeck, U., Kenner, L., Trajanoski, Z., Hoefler, G., Bogner-Strauss, J.G., 2011. Adipose triglyceride lipase and hormone-sensitive lipase are involved in fat loss in JunB-deficient mice. Endocrinology 152, 2678–2689.

Prentki, M., Matschinsky, F.M., Madiraju, S.R., 2013. Metabolic signaling in fuel-induced insulin secretion. Cell Metab. 18, 162–185.

Reverte-Salisa, L., Sanyal, A., Pfeifer, A., 2018. Role of cAMP and cGMP Signaling in Brown Fat. Handb. Exp. Pharmacol.

Roden, M., 2006. Mechanisms of Disease: hepatic steatosis in type 2 diabetes–pathogenesis and clinical relevance. Nat. Clin. Pract. Endocrinol. Metab. 2, 335–348.

Sepa-Kishi, D.M., Ceddia, R.B., 2018. White and beige adipocytes: are they metabolically distinct? Horm. Mol. Biol. Clin. Investig. 33.

Shostak, A., Meyer-Kovac, J., Oster, H., 2013. Circadian regulation of lipid mobilization in white adipose tissues. Diabetes 62, 2195–2203.

Sinha, A., Faller, D.V., Denis, G.V., 2005. Bromodomain analysis of Brd2-dependent transcriptional activation of cyclin A. Biochem. J. 387, 257–269.

Sun, R., Wu, Y., Hou, W., Sun, Z., Wang, Y., Wei, H., Mo, W., Yu, M., 2017. Bromodomain-containing protein 2 induces insulin resistance via the mTOR/Akt signaling pathway and an inflammatory response in adipose tissue. Cell. Signal. 30, 92–103.

Titchenell, P.M., Quinn, W.J., Lu, M., Chu, Q., Lu, W., Li, C., Chen, H., Monks, B.R., Chen, J., Rabinowitz, J.D., Birnbaum, M.J., 2016. Direct Hepatocyte Insulin Signaling Is Required for Lipogenesis but Is Dispensable for the Suppression of Glucose Production. Cell Metab. 23, 1154–1166.

Wang, F., Liu, H., Blanton, W.P., Belkina, A., Lebrasseur, N.K., Denis, G.V., 2009. Brd2 disruption in mice causes severe obesity without Type 2 diabetes. Biochem. J. 425, 71–83.

Wang, X., Yu, W., Nawaz, A., Guan, F., Sun, S., Wang, C., 2010. Palmitate induced insulin resistance by PKCtheta-dependent activation of mTOR/S6K pathway in C2C12 myotubes. Exp. Clin. Endocrinol. Diabetes 118, 657–661.

Wu, W., Wang, S., Xu, Z., Wang, X., Feng, J., Shan, T., Wang, Y., 2018. Betaine promotes lipid accumulation in adipogenic-differentiated skeletal muscle cells through ERK/PPARgamma signalling pathway. Mol. Cell. Biochem.

Yadav, A., Kataria, M.A., Saini, V., Yadav, A., 2013. Role of leptin and adiponectin in insulin resistance. Clin. Chim. Acta 417, 80–84.

Yang, Y., Yang, G., 2010. Rosiglitazone regulates IL-6-stimulated lipolysis in porcine adipocytes. Biochem. Cell Biol. 88, 853–860.

Zabielski, P., Hady, H.R., Chacinska, M., Roszczyc, K., Gorski, J., Blachnio-Zabielska, A.U., 2018. The effect of high fat diet and metformin treatment on liver lipids accumulation and their impact on insulin action. Sci. Rep. 8, 7249.

Zang, K., Wang, J., Dong, M., Sun, R., Wang, Y., Huang, Y., Liu, X., Li, Y., Wang, F., Yu, M., 2013. Brd2 inhibits adipogenesis via the ERK1/2 signaling pathway in 3T3-L1 adipocytes. PLoS ONE 8, e78536.

Zhang, S., Cao, H., Li, Y., Jing, Y., Liu, S., Ye, C., Wang, H., Yu, S., Peng, C., Hui, L., Wang, Y.C., Zhang, H., Guo, F., Zhai, Q., Wang, H., Huang, R., Zhang, L., Jiang, J., Liu, W., Ying, H., 2018a. Metabolic benefits of inhibition of p38alpha in white adipose tissue in obesity. PLoS Biol. 16, e2004225.

Zhang, S., Liu, G., Xu, C., Liu, L., Zhang, Q., Xu, Q., Jia, H., Li, X., Li, X., 2018b. Perilipin 1 Mediates Lipid Metabolism Homeostasis and Inhibits Inflammatory Cytokine Synthesis in Bovine Adipocytes. Front. Immunol. 9, 467.

Zhu, M., Liu, M., Guo, Q.L., Zhu, C.Q., Guo, J.C., 2018. Prolonged DADLE exposure epigenetically promotes Bcl-2 expression and elicits neuroprotection in primary rat cortical neurons via the PI3K/Akt/NF-kappaB pathway. Acta Pharmacol. Sin.